Hindawi
Advances in Materials Science and Engineering
Volume 2019, Article ID 2498916, 13 pages
https://doi.org/10.1155/2019/2498916

Research Article

A Stress-Strain Model for Unconfined Concrete in Compression considering the Size Effect

Keun-Hyeok Yang, Yongjei Lee, and Ju-Hyun Mun

Architectural Engineering, Kyonggi University, Suwon, Republic of Korea

Correspondence should be addressed to Ju-Hyun Mun; mjh@kgu.ac.kr

Received 29 September 2018; Revised 24 January 2019; Accepted 17 February 2019; Published 12 March 2019

Academic Editor: Hugo C. Biscaia

In this study, a stress-strain model for unconfined concrete with the consideration of the size effect was proposed. The compressive strength model that is based on the function of specimen width and aspect ratio was used for determining the maximum stress. In addition, in stress-strain relationship, a strain at the maximum stress was formulated as a function of compressive strength considering the size effect using the nonlinear regression analysis of data records compiled from a wide variety of specimens. The descending branch after the maximum stress was formulated with the consideration of the effect of decreasing area of fracture energy with the increase in equivalent diameter and aspect ratio of the specimen in the compression damage zone (CDZ) model. The key parameter for the slope of the descending branch was formulated as a function of equivalent diameter and aspect ratio of the specimen, concrete density, and compressive strength of concrete. Consequently, a rational stress-strain model for unconfined concrete was proposed. This model reflects trends that the maximum stress and strain at the peak stress decrease and the slope of the descending branch increases, when the equivalent diameter and aspect ratio of the specimen increase. The proposed model agrees well with the test results, irrespective of the compressive strength of concrete, concrete type, equivalent diameter, and aspect ratio of the specimen.

1. Introduction

The stress-strain relationship for unconfined concrete is a fundamental material property for the design and analysis of structural elements [1–3]. Generally, in stress-strain relationship, the ascending and descending branches are dependent on concrete type and compressive strength, as well as the maximum diameter of aggregate, specimen width or diameter, and aspect ratio in the descending branch from the crack propagation in the fracture zone [4–7]. The slope of the ascending branch commonly increases with the increase in compressive strength of concrete and the decrease in specimen width or diameter and aspect ratio, while that of the descending branch increases with concrete compressive strength, specimen width or diameter, and aspect ratio. To study this trend, researchers [5, 8–10] proposed concrete compressive strength models with the size effect in various approaches based on the fracture energy theory. Bažant and Planas [8] reported that concrete compressive strength was considerably affected by the specimen width or diameter, indicating that it decreased by 10%, when the specimen width or diameter increased twice. Sim et al. [5] emphasized that the size effect on compressive strength for lightweight concrete (LWC) was more notable than that for normal weight concrete (NWC). In particular, because cracks at the failure zone for LWC pass through lightweight aggregate particles, the crack band zone is more localized in LWC than NWC. Hence, the size effect of concrete on the peak stress and descending branch behavior that is directly related to crack propagations in the failure zone could be more notable in LWC than those in NWC [5]. However, for the size effect of concrete on the descending branch from the crack propagation in a localized crack band zone, only few studies have been conducted. In particular, very little literature on the size effect in LWC is available. Furthermore, the existing proposed models [6, 7] for the stress-strain relationship regarding the size effect of concrete on the descending branch are typically determined from NWC test

data records, rather than from LWC, with limited ranges of variables.

Markeset and Hillerborg [6] generalized the compression damage zone (CDZ) model to consider the size effect of concrete on the descending branch using a function of strain dissipated by the shear band including the fracture energy. However, the descending branch behavior in Markeset and Hillerborg's model are drawn from the limited ranges of variables. In addition, this model is limited for a practical equation because the specific information about the strain of the starting point for the softening behavior is not available. Samani and Attard [7] considered the size effect on the descending branch in stress-strain relationship proposed by Attard and Setunge's model [11], using the CDZ model [6]. As the Samani and Attard's [7] model has an identical strain model of shear band as that of Markeset and Hillerborg's [6], information regarding the material property factors is necessary to predict the stress-strain relationship. In addition, the descending branch of these models does not fully consider the effect of aggregate property on crack propagation and the localized fracture zone. For example, in LWC, the contribution of stress transfer at the crack plane for aggregate interlocking action is little [5] because most of the cracks at the failure plane pass through lightweight aggregate particles. In addition, the strength and elastic modulus of aggregates such as magnetite in heavyweight concrete (HWC) are typically higher than those in NWC, which can cause a wider fracture zone by crack propagation. Hence, the size effect of LWC and HWC could be different from that of NWC because the size effect on concrete depends on the areas of failure and crack propagation in the fracture zone. However, as the existing models [6, 7] incorporating the size effect of concrete on the descending branch were derived from limited NWC test data records, a limited number of studies for the size effect of concrete using lightweight and heavyweight aggregates are available.

The objective of this study is to propose a model for the stress-strain curve considering the size effect of various concrete types. In this model, the basic formula for the stress-strain curve and the key parameter that determines the slopes of the ascending and descending branches established by Yang et al. [1] was used to generate a complete nonlinear curve. The concrete compressive strength model proposed by Sim et al. [5] that considers the size effect was used for the peak stress. The strain at the peak stress was generalized with a simple equation using the regression analysis of data records compiled from specimens with various ranges of equivalent diameter and aspect ratio of specimen, compressive strength, and density. In the softening behavior of the descending branch in the stress-strain relationship, the size effect and fracture energy were considered using Markeset and Hillerborg's CDZ model [6]. The key parameter for the softening behavior was determined from the secant modulus joining the origin and $0.5f'_{SE}$, where f'_{SE} is the compressive strength of concrete considering the size effect. The strain model at $0.5f'_{SE}$ to determine the key parameter was generalized with various ranges of variables using nonlinear regression analysis. Finally, the key parameter that determines the slope of the descending branch was formulated as a function of equivalent diameter and aspect ratio of specimen, concrete density, and concrete compressive strength, using parametric numerical analysis. The accuracy of the proposed model was evaluated using a normalized root-mean-square error obtained from the comparisons of predicted curves with the test results.

2. Database

To formulate the material properties, Yang et al. [1] compiled 3295 data records for the elastic modulus of concrete (E_c), 415 data records for strain at the peak stress (ε_0), and 96 data records for strain at 50% of the peak stress ($\varepsilon_{0.5}$) in the descending branch. In the compiled data records, the numbers available for the concrete compressive strength (f'_c) and density (ρ_c) were 3295 and 3274, respectively, and varied from 8.4 MPa to 170 MPa and from 1200 kg/m^3 to 4500 kg/m^3, respectively. To apply the effect of concrete type to the empirical formulations, the data records were divided into LWC, NWC, and HWC according to ρ_c. The concrete density (ρ_c) varied from 1200 kg/m^3 to 2000 kg/m^3 for LWC, from 2000 kg/m^3 to 2500 kg/m^3 for NWC, and from 2500 kg/m^3 to 4500 kg/m^3 for HWC. The data records compiled by Yang et al. [1] were all measured from a cylinder of diameter 100 mm and height 200 mm. Hence, the data records compiled by Yang et al. [1] lack the test results for different specimen size. To compensate for this, additional test results for the size effect of concrete were compiled. The compiled additional test results [4, 5, 12–15] for the stress-strain relationship were 38 data records for LWC and 26 data records for NWC, as shown in Table 1. To consider various specimen shapes, an equivalent diameter ($d_{eq} \approx \sqrt{(4B\ D/\pi)}$) was introduced, where B and D are the sectional width and depth of prism specimen, respectively, assuming that the area of the prism specimens is identical to that of cylinder specimen. For example, for prism specimens with a B of 300 mm and D of 400 mm, d_{eq} corresponds to 398.9 mm. In the data records, d_{eq}, aspect ratio (h/d_{eq}), f'_c, and ρ_c were varied from 50 mm to 800 mm, 0.5 to 8, 4 mm to 20 mm, 17.1 MPa to 90.2 MPa, and 1500 kg/m^3 to 2464 kg/m^3, respectively. The specimen equivalent diameter (d_{eq}) and h/d_{eq} were varied from 100 mm to 350 mm and 1 to 2 for LWC and 50 mm to 800 mm and 0.5 to 8 for NWC, respectively.

3. Model Generalization

3.1. Basic Approach. The stress-strain relationship for unconfined concrete in compression is a parabola with ascending and descending branches, and a vertex at the peak stress [1–3]. This shape can be generalized using the following equation [1]:

$$y = \frac{(\beta_1 + 1)x}{x^{\beta_1+1} + \beta_1}, \tag{1}$$

where $y = f_c/f'_c$ is the normalized stress, $x = \varepsilon_c/\varepsilon_0$ is the normalized strain, f_c and ε_c are the concrete stress and strain at some point in stress-strain curve, respectively, and β_1 is the key parameter that determines the slopes of the ascending and descending branches. The ascending branch

Table 1: Distribution of parameters in the data records for stress-strain curves.

f'_c (MPa)	Range	<20	20–40	40–60	60–80	80–100	Total
	LWC	4	26	8	0	0	38
	NWC	2	3	16	0	5	26
d_{eq} (mm)	Range	<50	50–100	100–200	200–300	>400	Total
	LWC	0	34	1	2	1	38
	NWC	3	19	3	0	1	26
h/d_{eq}	Range	0.5-1	1-2	2-3	3–5	5–8	Total
	LWC	3	35	0	0	0	38
	NWC	4	8	3	6	5	26
d_a (mm)	Range	4	4–10	10–15	15–20	>20	Total
	LWC	1	2	2	33	0	38
	NWC	0	14	0	12	0	26

can be determined from E_c, which is defined as the slope of the line joining the origin and 40% of the peak stress [16]. In addition, the descending branch can be determined from the secant modulus joining the origin and $0.5f'_c$ [1]. In accordance with Yang et al.'s model [1], the equation for the key parameter β_1 that determines the slopes of the ascending and descending branches can be expressed in the following forms:

$$\begin{aligned} 0.4(X_a)^{\beta_1+1} + (0.4 - X_a)\beta_1 - X_a = 0, \quad & \text{for } \varepsilon_c \le \varepsilon_0, \\ (X_d)^{\beta_1+1} + (1 - 2X_d)\beta_1 - 2X_d = 0, \quad & \text{for } \varepsilon_c > \varepsilon_0, \end{aligned} \tag{2}$$

where $X_a = 0.4f'_c/E_c\varepsilon_0$ and $X_d = \varepsilon_{0.5}/\varepsilon_0$.

Bažant [9] proposed the crack band zone by a crack width with microcrack propagation for concrete failure. In addition, Bažant [9] idealized the crack band width as a function of d_a, assuming that microcracks propagated the interfaces between aggregates and pastes. Sim et al. [5] proposed a smaller area of the crack band zone in LWC than NWC as shown in Figure 1, based on the crack band theory [9]. This model includes the effect of reduced area of the crack band zone caused by the cracks at the failure zone passing through lightweight aggregate particles and also considers the size effect on concrete due to the decrease in α/d_{eq} as d_{eq} increases, where α is the crack length. The above previous models clearly revealed that the size effect exists in compressive strength of concrete due to different propagations of longitudinal splitting cracks at different specimen sizes, although further elaborated analytical approach would be needed to account for the effect of splitting cracks on the size effect in different concrete types. Sim et al. [5] derived the equation for the compressive strength of concrete (f'_{SE}) considering the size effect from the energy balance up to the peak stress in the crack band zone idealizing the propagation of longitudinal splitting cracks, in that the strain energy for concrete deformation dissipated by the crack band zone equals the total energy consumed by the band of the axial microsplitting cracks. The proposed model is as follows:

$$f'_{SE} = \left[\frac{A_1\sqrt{(1/k)\left(h/d_{eq}\right)^{X_4}}}{\left[1 + \left(B_1\left(d_{eq}/d_a^{X_1}\right)\left(\rho_c/2300\right)^{-X_2}\right)\right]^{0.5}}\right] f'_c, \tag{3}$$

where A_1 is $\sqrt{(nk_1X_3/F_2)(1 - (E_c/E_t))}$, n is the number of microcracks in the band, B_1 is F_1/F_2, F_1 is $\partial F/\partial\alpha_1$, F_2 is $\partial F/\partial\alpha_2$, F is $f(\alpha_1, \alpha_2)$, α_1 and α_2 are the modification factors to account for the volume of the crack band zone, E_t is the strain-softening modulus, and X_1, X_2, X_3, and X_4 are the experimental constants. In equation (3), f'_c indicates the compressive strength of concrete measured in a reference specimen with d of 150 mm and h/d_{eq} of 2. From equation (3), this indicates that f'_c is considerably affected by the functions of d_{eq}, h/d_{eq}, and ρ_c [5, 8–10]. Sim et al. [5] determined the functions of A_1, B_1, $d_a^{X_1}$, k, X_2, and X_4 in equation (3) from 1509 data records with LWC and NWC test results and proposed as follows:

$$f'_{SE} = \left[\frac{0.9\sqrt{\left(h/d_{eq}\right)^{-0.6}}}{\left[1 + 0.017d_{eq}\left(\rho_c/2300\right)^{-1}\right]^{0.5}} + 0.63\right] f'_c. \tag{4}$$

In the model of Sim et al. [5], equation (4) considers a function of ρ_c that reflects the trend that the size effect is more notable in LWC than that in NWC. The stress-strain relationship is shown in Figure 2, using equation (4) for the peak stress. In Figure 2, the key parameter β_1 can be determined with the following equations:

$$0.4(X_{a1})^{\beta_1+1} + (0.4 - X_{a1})\beta_1 - X_a = 0, \quad \text{for } \varepsilon_c \le \varepsilon_{SE}, \tag{5}$$

$$(X_{d1})^{\beta_1+1} + (1 - 2X_{d1})\beta_1 - 2X_{d1} = 0, \quad \text{for } \varepsilon_c > \varepsilon_{SE}, \tag{6}$$

where $X_{a1} = 0.4f'_{SE}/E_c\varepsilon_{SE}$, $X_{d1} = \varepsilon_{SE0.5}/\varepsilon_{SE}$, ε_{SE} is the strain at the peak stress considering the size effect, and $\varepsilon_{SE0.5}$ is the strain at $0.5f'_{SE}$ after the peak stress. In equation (1), the key parameter β_1 that determines the ascending and descending branches requires information about the functions of E_c, ε_{SE}, and $\varepsilon_{SE0.5}$, as expressed in equations (5) and (6).

3.2. Determination of β_1 in Ascending Branch. The size effect on concrete is based on the crack band theory indicating the crack width with the propagation of microcracks, as shown in Figure 3. It implies that the behavior of the points of "O" and "A" without any cracks in the graph is not affected by the size effect. In addition, Taylor and Broms [17] reported that the bond cracks can be definitely observed between 38 and 42% of the peak stress at the ascending branch of the stress-strain curve. As a result, the strain at the ascending branch begins to increase rapidly with the propagation of the bond cracks, showing the nonlinear curve, as pointed out by Neville [16]. According to fracture mechanics, the size effect on concrete is primarily caused by the crack propagation. Thus, the present study considered that E_c representing the quasi-linear relationship at the ascending branch is marginally affected by the size effect. Yang et al. [1] formulated the empirical formulation for E_c on the basis of the regression analysis of 2680 data records for NWC, 370 data records for LWC with ρ_c ranging from 1200 to 2000 kg/m^3, and 245 data records for HWC with ρ_c ranging from 2500 to 4450 kg/m^3. Noguchi et al. [18] reported that E_c can be expressed as a function of f'_c and ρ_c and included correction factors to account for the effects of aggregate type and presence of supplementary cementitious materials (SCMs). In Yang et al.' model [1], the various unusual aggregates such

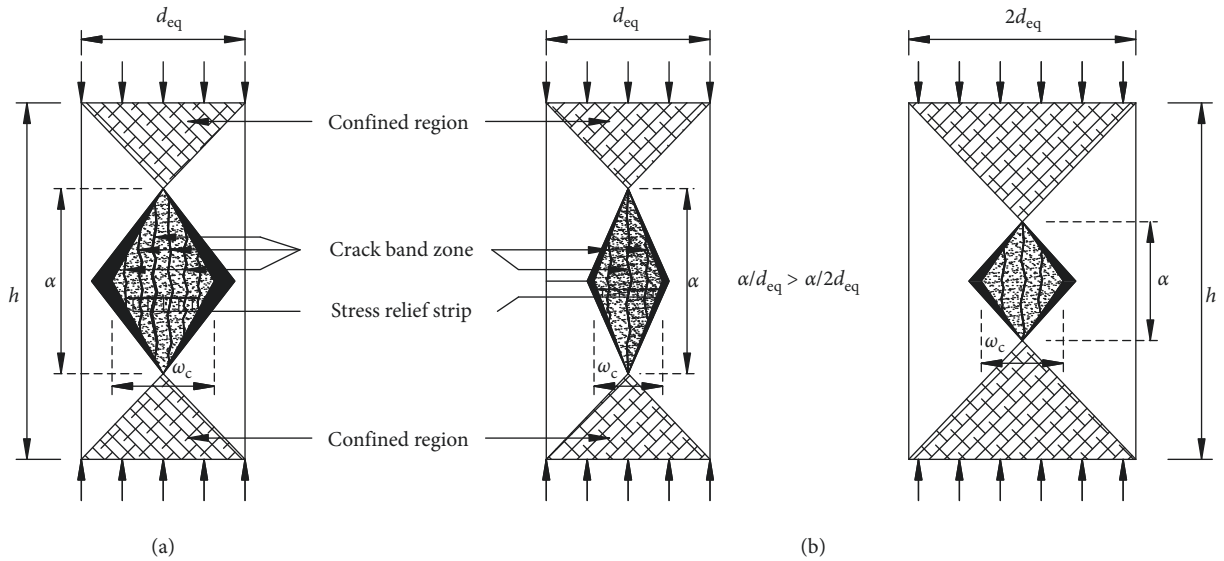

Figure 1: Idealized crack band zone at peak stress based on concrete fracture mechanics. (a) NWC. (b) LWC.

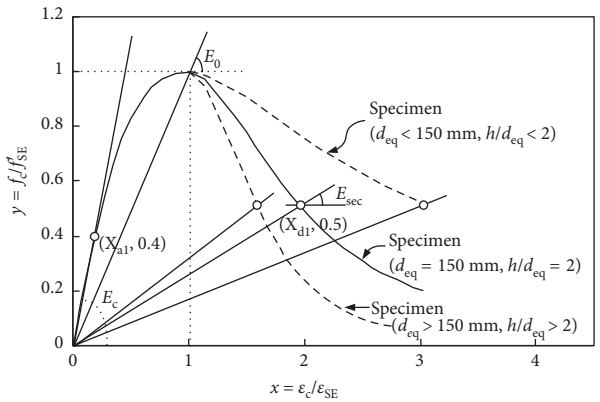

Figure 2: Generalization of the compressive stress-strain curve of concrete considering the size effect.

as artificial lightweight aggregates and heavyweight magnetite particles were implicitly considered in the use of the parameter of ρ_c. In addition, the correction factor for SCMs can be implicitly included when the empirical constants are obtained from regression analysis, resulting in negligible errors. Yang et al.'s model reflected the trend that a lower increasing rate in E_c than that in f_c' was considered by using a power function of f_c' to represent the nonlinear relationship between the two parameters. Consequently, Yang et al.'s model [1] was used for E_c as follows:

$$E_c = 8470\left(f_c'\right)^{1/3}\left(\frac{\rho_c}{2300}\right)^{1.17}. \tag{7}$$

Meanwhile, as shown in Figure 2, equation (4) can be expressed as follows from the relation of f_{SE}' and E_0:

$$\varepsilon_{SE} = \left[\frac{0.9\sqrt{\left(h/d_{eq}\right)^{-0.6}}}{\left[1 + 0.017d_{eq}\left(\rho_c/2300\right)^{-1}\right]^{0.5}} + 0.63\right]\frac{f_c'}{E_0}. \tag{8}$$

Consequently, ε_{SE} can be expressed as follows:

$$\varepsilon_{SE} = \frac{f_{SE}'}{E_0}, \tag{9}$$

where E_0 is the secant modulus joining the origin and the peak stress. Equation (9) shows that ε_{SE} is fully affected by the functions of f_{SE}' and E_0. However, data records or predicted model for E_0 is not available in the literature. Hence, in this study, E_0 can be proposed as follows using a certain relation with E_c, as shown in Figure 2:

$$\varepsilon_{SE} = \chi\left(\frac{f_{SE}'}{E_c}\right), \tag{10}$$

where χ is a coefficient to account for the relation of E_0 and E_c, which can be determined from the test results. From the data records compiled in this study, equation (10) can be proposed as follows (Figure 4):

$$\varepsilon_{SE} = 0.0016\ \exp\left[220\left(\frac{f_{SE}'}{E_c}\right)\right]. \tag{11}$$

The key parameter β_1 that determines the slope of the ascending branch can be solved by substituting equations (7) and (11) into equation (5). The key parameter β_1 was calculated using the Newton–Raphson method, identical to Yang et al.'s model [1]. The β_1 values determined for different concrete properties need to be formulated as a simple equation for practical application of the proposed stress-strain relationship of concrete. Thus, the present research involved a parametric study to generalize β_1 under the comprehensive ranges of parameters as follows: f_c' between 10 MPa and 180 MPa; ρ_c between 1400 kg/m^3 and 4000 kg/m^3; d_{eq} between 50 mm and 500 mm; and h/d_{eq} between 0.5 and 5. Note that the geometrical conditions of specimens were considered in the parametric study because the given parameters in equations (4) and (11) are affected by the equivalent width and aspect ratio of the specimen. From the regression analysis using the solutions

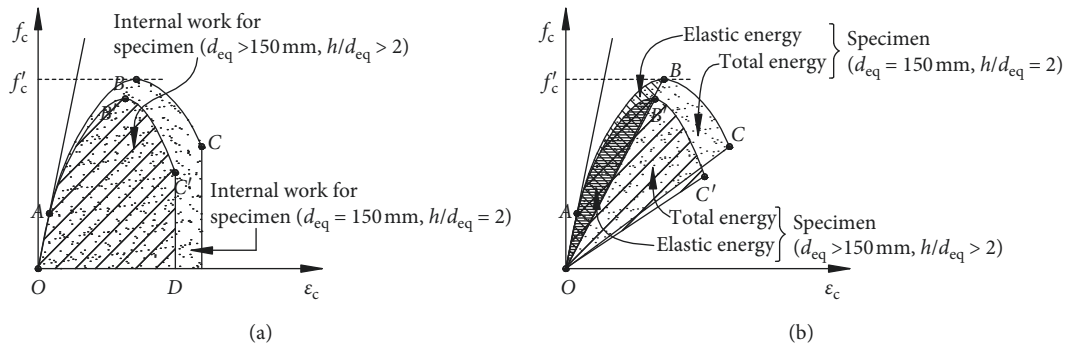

Figure 3: Fracture energy for concrete failure.

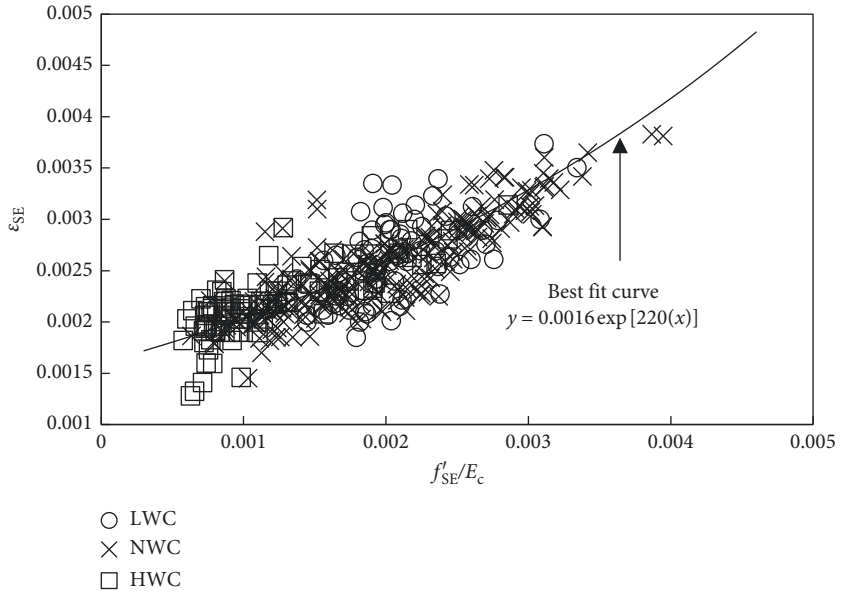

Figure 4: Nonlinear regression analysis for ε_{SE}.

obtained from the Newton–Raphson method, the key parameter β_1 to account for the slope of the ascending branch can be simply formulated as follows (Figure 5):

$$\beta_1 = 0.33 \exp\left[0.42\left(\frac{f'_{SE}}{10}\right)\left(\frac{2300}{\rho_c}\right)^{1.5}\right], \quad \text{for } \varepsilon_c \le \varepsilon_{SE}. \tag{12}$$

Equation (12) shows that the slope of the ascending branch increases with the increase in f'_{SE} or decrease in ρ_c. Consequently, the slope of the ascending branch includes the size effect of concrete with the generalization of a function of f'_{SE}, considering the parameters d_{eq} and h/d_{eq}.

3.3. Determination of β_1 in Descending Branch. The compressive failure behavior of unconfined concrete is commonly characterized by the mode I (pure tensile) and mode III (sliding displacement due to diagonal shear) in estimating the fracture zone. As pointed out by Markeset and Hillerborg, microsplitting cracks (mode I) are formulated due to Poisson's effect under pure compressive stresses, whereas sliding displacement along diagonal tensile cracks (mode III) occurs at

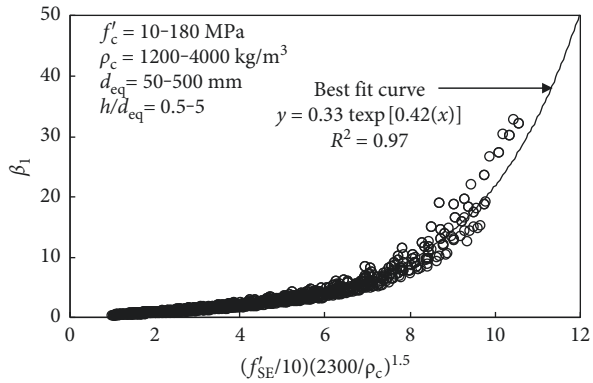

Figure 5: Formulation of key parameter β_1 in the ascending branch in stress-strain relationship.

45-degree slope relative to the principal normal stresses when the maximum shearing stresses reach the shear capacity of concrete. Hence, Markeset and Hillerborg assumed that longitudinal crack zones of concrete relate to the tensile fracture energy zone, whereas diagonal shear crack zones after

the peak stress identify the shear fracture energy zone (Figure 6). In fact, most of cracks in concrete are caused by tensile stresses rather than compressive stresses because the tensile resistance of concrete is highly lower than the compressive resistance. Overall, the compressive failure of concrete is commonly caused by the tensile fracture due to Poisson's effect. The descending branch behavior after the peak stress is determined from the localized deformation developed in the damaged or failure zone, while the undamaged zone elastically unloads [6]. Hence, the undamaged zone is generated only when h is greater than the damaged zone height (h_d). For compressive behavior, Markeset and Hillerborg [6] idealized the CDZ model generated from the longitudinal microsplitting cracks and localized diagonal tensile shear band crack in the damaged zone (Figure 6). In CDZ model, microsplitting cracks can be idealized as a crack band zone with several microsplitting cracks because their propagation requires energy release. Thus, the size effect of concrete on compression is expected as demonstrated by lots of previous researches. Bažant and Planas also idealized the fracture energy zone of concrete under compression, considering the tensile and diagonal shear cracks to consider the size effect. According to Markeset and Hillerborg [6], the total strain ε_c in the softening behavior is the sum of the strain during the unloading region after the peak stress in the undamaged zone, the strain while microsplitting crack occurs in the longitudinal direction, and the strain caused by the diagonal shear band (ω/h):

$$\varepsilon_c = \varepsilon + \varepsilon_d\left(\frac{h_d}{h}\right) + \frac{\omega}{h}, \quad \text{for } h > h_d, \tag{13a}$$

$$\varepsilon_c = \varepsilon + \varepsilon_d + \frac{\omega}{h}, \quad \text{for } h \le h_d, \tag{13b}$$

where h_d is the height of the region propagated by the longitudinal microsplitting cracks. ω is the localized deformation assumed between 0.4 and 0.7 for NWC and less than 0.3 for LWC. The longitudinal microsplitting cracks in unconfined concrete under compression commonly develop at approximately 75~90% of the peak stress. From this finding, in the CDZ model, the amount of energy (W^{in}) released in the unloading zones can be obtained using the following equation:

$$W^{in} = \frac{G_F}{\gamma(1+k)}, \tag{14}$$

where G_F is the fracture energy and k is the factor based on the material properties. γ is the factor to account for average spacing between longitudinal spitting microcracks. Assuming that the strain (ε_d) in the region propagated by the longitudinal microsplitting cracks is proportional to the tensile fracture energy (G_F), it can be proposed as follows:

$$\varepsilon_d = \left[\frac{2kG_F}{\gamma(1+k)f_c'}\right]\left(\frac{f_c' - f_c}{f_c'}\right)^{0.8}. \tag{15}$$

As expressed in equation (15), the CDZ model proposed by Markeset and Hillerborg [6] includes a function of G_F, in the descending branch. However, G_F, k, and ω require calibration according to various concrete types because they are based on the material properties, which are too demanding for a practical application. Furthermore, because γ is proposed only for a d_a of 16 mm, the use of a practical equation is limited for other specimens with larger aggregate. Hence, to obtain information about these factors, a comprehensive test is required with various influencing parameters including concrete type, d_{eq}, h/d_{eq}, and d_a. To improve Markeset and Hillerborg's model [6], the key parameter β_1 by Yang et al. [1] was applied to the descending branch behavior. The peak stress from equation (4) by Sim et al. [5] and $\varepsilon_{SE0.5}$ from equations (13a) and (13b) are used to produce the following equation:

$$\varepsilon_{SE0.5} = \left(\varepsilon_{SE} - \frac{f_{SE}'}{E_c}\right) + \left(\frac{2kG_F}{\gamma(1+k)f_{SE}'}\right) \cdot \left(\frac{f_{SE}' - 0.5f_{SE}'}{f_{SE}'}\right)^{0.8}\frac{h_d}{h} + \frac{\omega}{h}, \quad \text{for } h > h_d, \tag{16a}$$

$$\varepsilon_{SE0.5} = \left(\varepsilon_{SE} - \frac{f_{SE}'}{E_c}\right) + \left(\frac{2kG_F}{\gamma(1+k)f_{SE}'}\right) \cdot \left(\frac{f_{SE}' - 0.5f_{SE}'}{f_{SE}'}\right)^{0.8} + \frac{\omega}{h}, \quad \text{for } h \le h_d, \tag{16b}$$

where ε_{SE}, E_c, and f_{SE}' are known values. In equations (16a) and (16b), the first term in the right is moved to the left side and can be arranged as follows:

$$\varepsilon_{SE0.5} - \left(\varepsilon_{SE} - \frac{f_{SE}'}{E_c}\right) = \left(\frac{2kG_F}{\gamma(1+k)f_{SE}'}\right)\left(0.5^{0.8}\right)\frac{h_d}{h} + \frac{\omega}{h}, \quad \text{for } h > h_d, \tag{17a}$$

$$\varepsilon_{SE0.5} - \left(\varepsilon_{SE} - \frac{f_{SE}'}{E_c}\right) = \left(\frac{2kG_F}{\gamma(1+k)f_{SE}'}\right)\left(0.5^{0.8}\right) + \frac{\omega}{h}, \quad \text{for } h \le h_d, \tag{17b}$$

where the values of k and γ are experimental constants in predicting the softening in the CDZ model. On the basis of test results, Markeset and Hillerborg assumed the value of k as 3.0 for NWC and 1.0 for LWC. However, the value of k for HWC is still unknown because of the lack of test data. Markeset and Hillerborg also introduced the factor γ to account for the average spacing of the longitudinal microsplitting cracks due to the primary tensile stresses. They assumed the value of γ as 1.25 for the maximum aggregate size of 16 mm. However, there is no further information on the value of γ for different aggregate sizes although the spacing of the longitudinal microsplitting cracks can be significantly affected by the aggregate size due to the aggregate interlock action. In addition, the value of γ depends on the equivalent width and aspect ratio of the specimen because the energy release at the crack band zone is affected by the spacing of the longitudinal microsplitting cracks.

The present study conducted the regression analysis of test data on $\varepsilon_{SE0.5}$ to simply generalize the right-hand side of equations (17a) and (17b) including the factors k and γ. Test

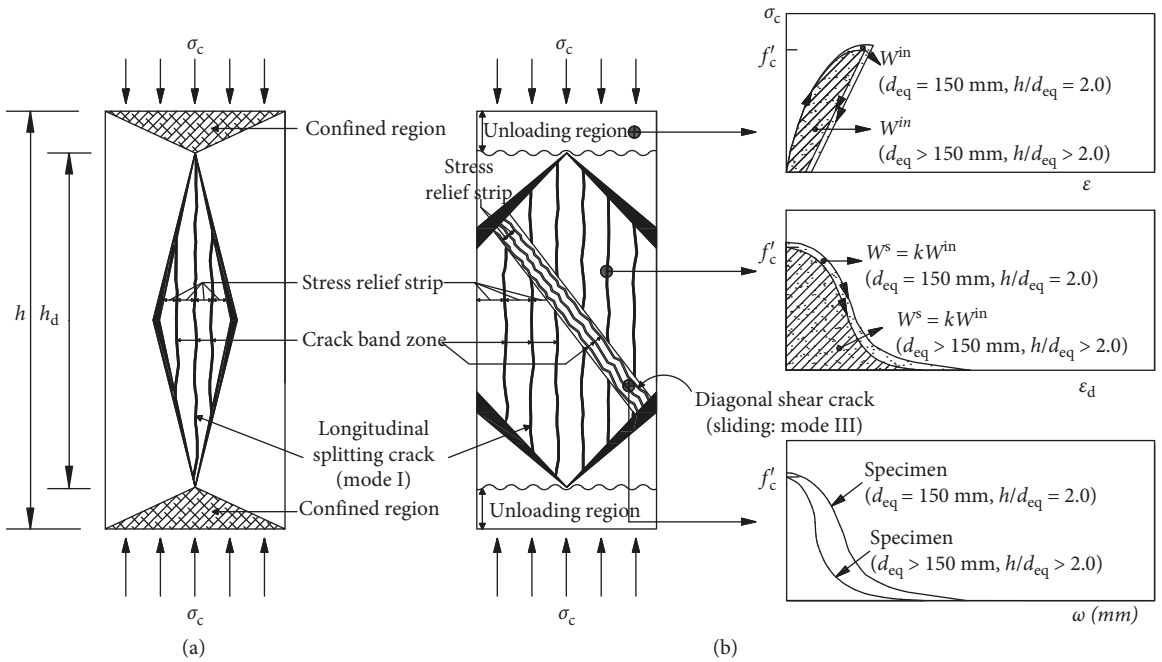

Figure 6: Compression damage zone (CDZ) model. (a) Ascending branch. (b) Descending branch.

results of $\varepsilon_{SE0.5} - (\varepsilon_{SE} - (f'_{SE}/E_c))$ according to d_{eq}, h/d_{eq}, and ρ_c are shown in Figure 7. In Figure 7(a), $\varepsilon_{SE0.5} - (\varepsilon_{SE} - (f'_{SE}/E_c))$ nonlinearly decreased with the increase in d_{eq}, indicating that it decreased by approximately 18% for specimens with h/d_{eq} of 2, and approximately 31% for specimens with h/d_{eq} of 1, when d_{eq} increased by 3 times. $\varepsilon_{SE0.5} - (\varepsilon_{SE} - (f'_{SE}/E_c))$ almost linearly decreased with h/d_{eq} increased, irrespective of f'_c. $\varepsilon_{SE0.5} - (\varepsilon_{SE} - (f'_{SE}/E_c))$ ranged between 0.0026 and 0.0049 for specimens with h/d_{eq} of 2 and 0.0018 for specimens with h/d_{eq} of 5.5, indicating that it decreased by 43%, when h/d_{eq} increased by 3 times. In addition, $\varepsilon_{SE0.5} - (\varepsilon_{SE} - (f'_{SE}/E_c))$ increased with the increase in ρ_c, and its increasing rate according to f'_c was almost constant. $\varepsilon_{SE0.5} - (\varepsilon_{SE} - (f'_{SE}/E_c))$ ranged between 0.002 and 0.0038 for LWC (ρ_c less than 2000 kg/m^3) and 0.0029 to 0.0044 for HWC (ρ_c more than 2500 kg/m^3). These imply that the descending branch behavior in the stress-strain relationship for unconfined concrete is considerably affected by the functions of d_{eq}, h/d_{eq}, and ρ_c. Based on this analysis, $\varepsilon_{SE0.5} - (\varepsilon_{SE} - (f'_{SE}/E_c))$ was generalized as functions of G_F, f'_{SE}, h/d_{eq}, and ρ_c (Figure 8), using regression analysis from the test results [4, 5, 12–15, 19–29] for 45 data records for LWC, 91 data records for NWC, and 24 data records for HWC:

$$\varepsilon_{SE0.5} - \left(\varepsilon_{SE} - \frac{f'_{SE}}{E_c}\right) = 0.0027 \exp\left[1.9 \times 1000\left(\frac{G_F^{0.4}}{f'^{1.4}_{SE} d_{eq}^{0.6}}\left(\frac{h}{d_{eq}}\right)^{-1.2} \cdot \left(\frac{\rho_c}{2300}\right)^2\right)\right], \tag{18}$$

where the CEB-FIP model [30] for G_F that includes functions of d_a and f'_c was expressed as follows:

$$G_F = G_{F0}\left(\frac{f'_c}{10}\right)^{0.7}, \tag{19}$$

where G_{F0} is 0.025 N/mm, 0.03 N/mm, and 0.05 N/mm for d_a of 8 mm, 16 mm, and 32 mm, respectively. Overall, the present model can predict the softening performance of concrete with different parameters including the compressive strength and density of concrete, equivalent width and aspect ratio of specimens, and aggregate sizes even though the values for k and γ are not determined from test specimens. The value of β_1 in the descending branch can be solved using equations (11) and (18). The solution of β_1 in the descending branch was also calculated using the Newton–Raphson method as in the ascending branch. Finally, the key parameter β_1 was formulated using the analytical parametric study. In the analytical parametric study, f'_c, d_{eq}, h/d_{eq}, d_a, and ρ_c were selected from 10 MPa to 180 MPa, 50 mm to 500 mm, 0.5 to 5, 4 mm to 25 mm, and 1400 kg/m^3 to 4000 kg/m^3, respectively. From the analytical results, statistical optimization was performed to generalize the key parameter β_1 that determines the slope of the descending branch as follows (Figure 9):

$$\beta_1 = 0.83\left[\left(\frac{f'_{SE}}{10}\right)^{0.65}\left(\frac{d_{eq}}{150}\right)^{0.2}\left(\frac{h}{d_{eq}}\right)^{0.4}\left(\frac{2300}{\rho_c}\right)^{1.2}\right]^{1.3}, \quad \text{for } \varepsilon_c > \varepsilon_{SE}. \tag{20}$$

Finally, the stress-strain relationship for unconfined concrete can be proposed as follows:

$$f_c = \left[\frac{(\beta_1 + 1)(\varepsilon_c/\varepsilon_{SE})x}{(\varepsilon_c/\varepsilon_{SE})^{\beta_1+1} + \beta_1}\right] f'_{SE}, \tag{21}$$

where ε_{SE} is given by equation (11), f'_{SE} is given by equation (4), and key parameter β_1 is given by equation (12) or (20). The proposed stress-strain relationship for unconfined

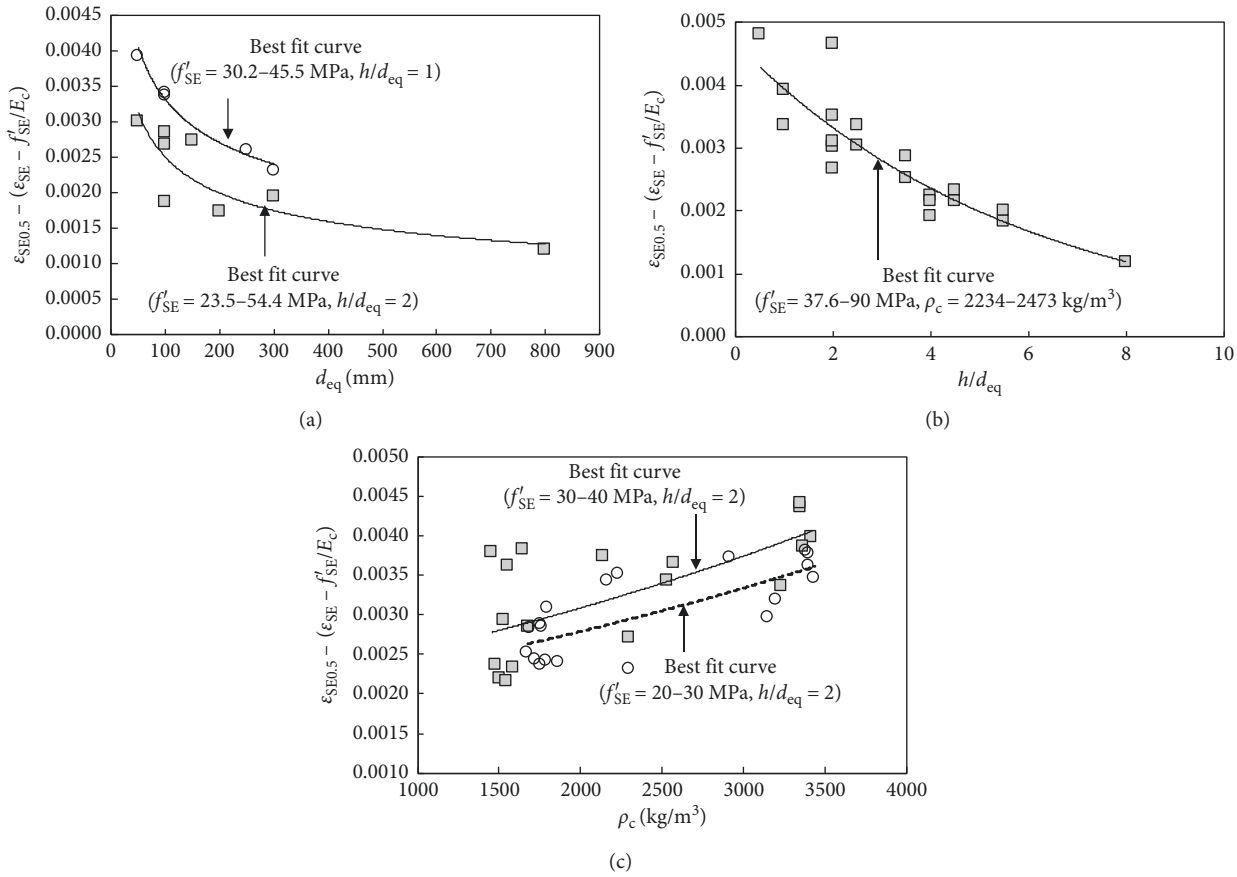

Figure 7: Variation in $\varepsilon_{SE0.5}$ in softening behavior. (a) Equivalent diameter d_{eq}. (b) Aspect ratio h/d_{eq}. (c) Concrete density ρ_c.

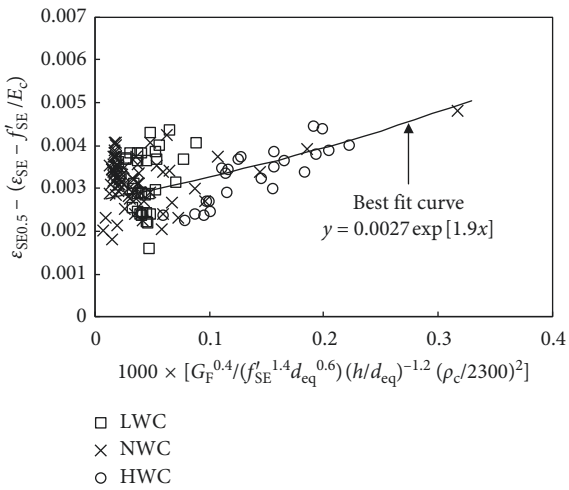

Figure 8: Nonlinear regression analysis to determine $\varepsilon_{SE0.5}$.

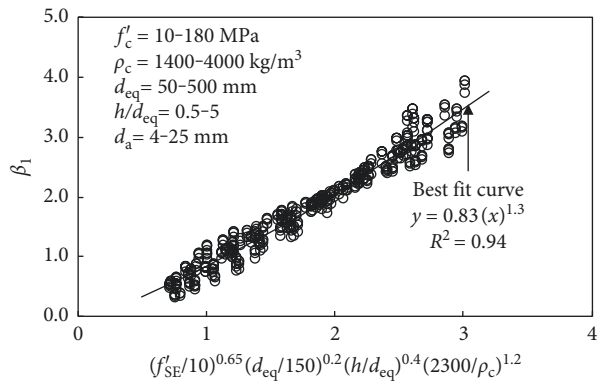

Figure 9: Formulation of key parameter β_1 in the descending branch in stress-strain relationship.

concrete can consider the size effect on concrete in the ascending and descending branches, using the power functions of the key parameters β_1 and f'_{SE}.

4. Comparisons with Test Results

The test results compiled from the available literatures [4, 5, 12–15, 19–29] were compared with predictions of this study and the existing models [1, 6, 7, 11]. The existing models for the strain-stress relationship proposed by Markeset and Hillerborg [6] and Samani and Attard [7] were selected as summarized in Table 2. Figure 10 shows comparisons of the predicted and measured stress-strain curves [4, 19–25]. The comparative analysis focused on the effect of d_{eq}, h/d_{eq}, ρ_c, and f'_c on the stress-strain curve. Table 3 summarizes the normalized root-mean-square error (NRMSE) obtained from the comparisons of test results with predictions. In Table 3, γ_m and γ_s are the mean and standard

Table 2: Summary of stress-strain models considering the size effect.

Researcher		Stress-strain relationship of concrete
Markeset and Hillerborg [6]	Ascending branch	—
	Descending branch	$\varepsilon_h = \varepsilon_0 - (f'_c/E_c) + \varepsilon_d((2.5d)/h) + (\omega/h)$, for h > 2d $\varepsilon_h = \varepsilon_0 - (f'_c/E_c) + \varepsilon_d + (\omega/h)$, for $h \le 2$d $\varepsilon_d = (2kG_F/\gamma(1+k)f'_c)((f'_c - f_c)/f'_c)^{0.8}$ $G_F = 0.00097f'_c + 0.0418$
Samani and Attard [7]	Ascending branch	$f_c = [(A(\varepsilon_c/\varepsilon_0) + B(\varepsilon_c/\varepsilon_0)^2)/(1 + ((A-2)(\varepsilon_c/\varepsilon_0)) + ((B+1)(\varepsilon_c/\varepsilon_0)^2))]f'_c$ $A = E_c\varepsilon_0/f'_c$; $B = ((A-1)^2/0.55) - 1$ $E_c = (3320\sqrt{f'_c} + 6900)(\rho_c/2300)^{1.5}$ $f_c = [(f_{ic}/f'_c)^{((\varepsilon_h - \varepsilon_0)/(\varepsilon_{ic} - \varepsilon_0))^2}]f'_c$ $\varepsilon_{ic} = [2.76 - 0.35\ln(f'_c)]\varepsilon_0$; $f_{ic} = [1.41 - 0.17\ln(f'_c)]f'_c$
	Descending branch	$\varepsilon_h = \varepsilon_0 + ((\varepsilon_c - \varepsilon_0)(h_0/h)) + (((f_c - f'_c)/E_c)[1 - (h_0/h)]) + \varepsilon_d((2d_{eq} - h_0)/h)$, for $h > 2d_{eq}$ $\varepsilon_h = \varepsilon_0 + ((\varepsilon_c - \varepsilon_0)(h_0/h)) + (((f_c - f'_c)/E_c)[1 - (h_0/h)]) + \varepsilon_d(1 - (h_0/h))$, for $h \le 2d_{eq}$ $\varepsilon_d = (2kG_F/\gamma(1+k)f'_c)((f'_c - f_c)/f'_c)^{0.8}$ $G_F = 0.00097f'_c + 0.0418$
		$\varepsilon_0 = (f'_c/E_c)(\mu_1/\sqrt[4]{f'_c})$ $\mu_1 = 4.26$ for crushed aggregates, and 3.78 for gravel aggregates.
This study		$f_c = (((\beta_1 + 1)(\varepsilon_c/\varepsilon_{SE})x)/((\varepsilon_c/\varepsilon_{SE})^{\beta_1+1} + \beta_1))f'_{SE}$ $f'_{SE} = (((0.9\sqrt{(h/d_{eq})^{-0.6}})/[1 + 0.017d_{eq}(\rho_c/2300)^{-1}]^{0.5}) + 0.63)f'_c\varepsilon_{SE} = 0.0016\exp[220(f'_c/E_c)]$ $E_c = 8470(f'_c)^{1/3}(\rho_c/2300)^{1.17}$
	Ascending branch	$\beta_1 = 0.33\exp[0.42(f'_{SE}/10)(2300/\rho_c)^{1.5}]$
	Descending branch	$\beta_1 = 0.83[(f'_{SE}/10)^{0.62}(d/150)^{0.2}(h/d)^{0.35}(2300/\rho_c)^{1.2}]^{1.3}$

f_c, f'_c, f'_{SE}, and E_c are in MPa; d_{eq}, h, h_0, ω, and γ are in mm; G_F is in N/mm; ρ_c is in kg/m^3.

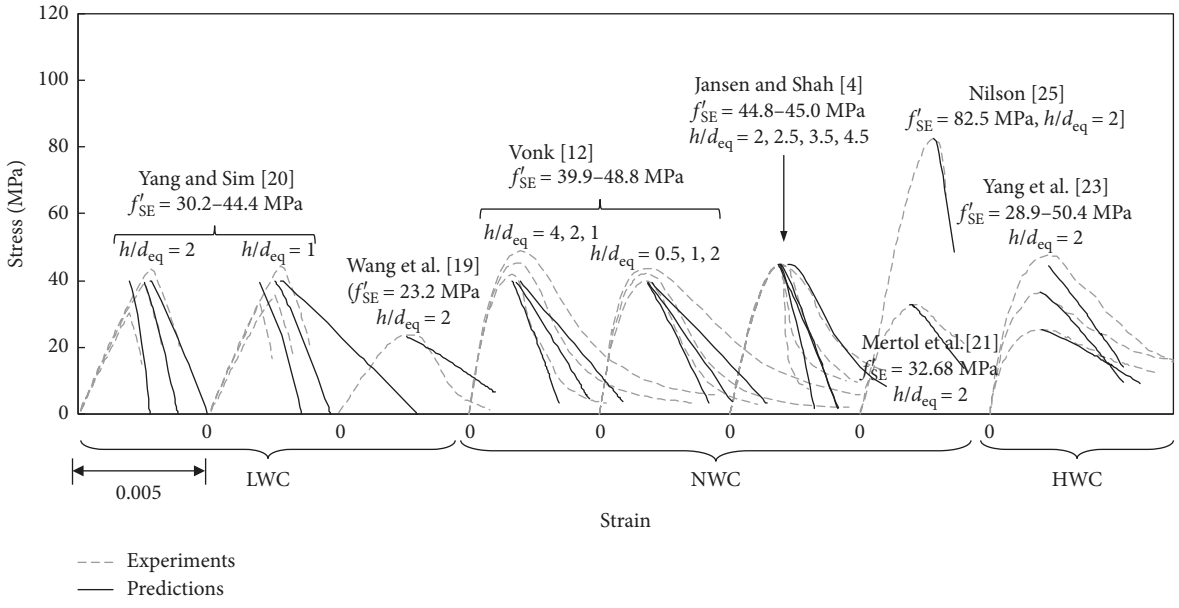

(a)

Figure 10: Continued.

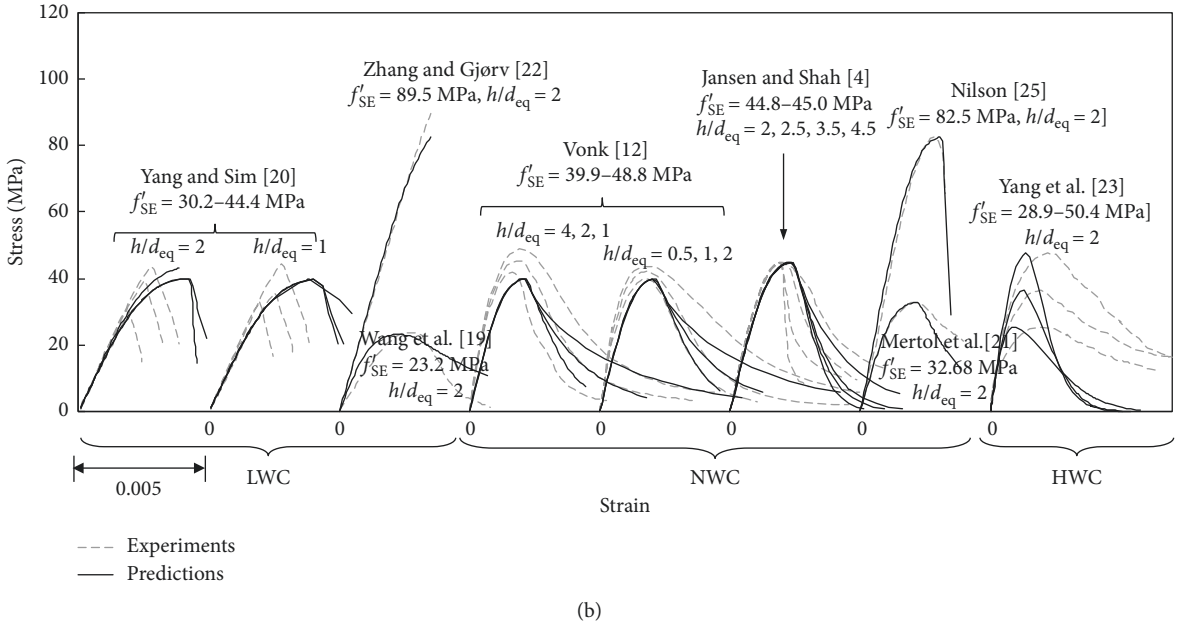

(b)

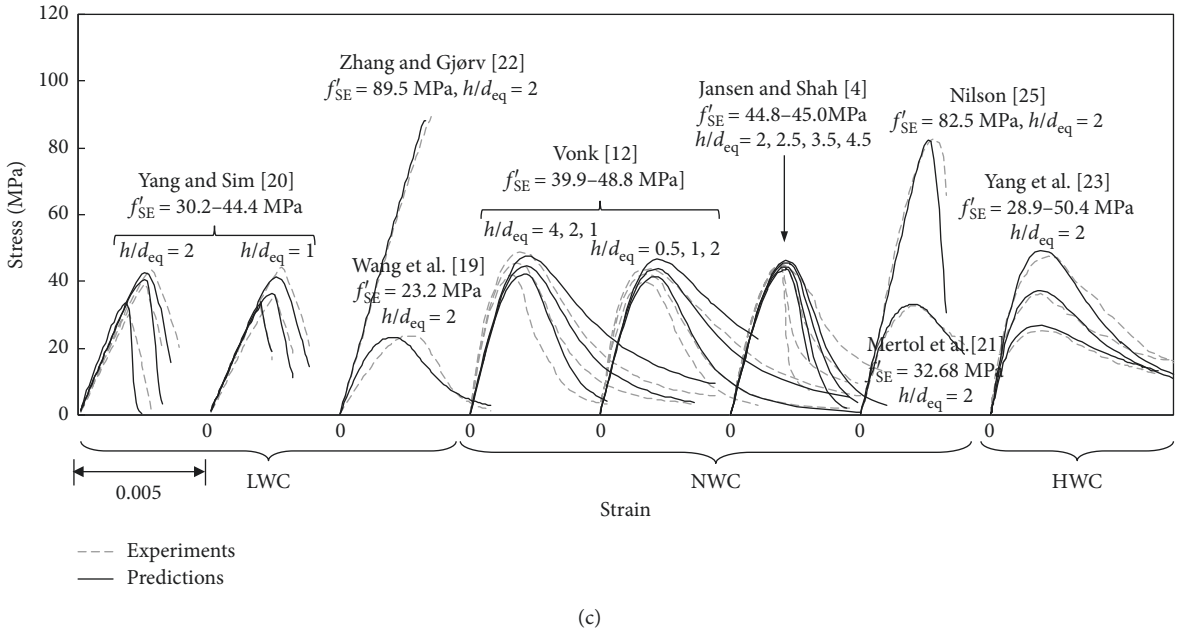

(c)

Figure 10: Typical comparisons of predicted and measured stress-strain curves. (a) Markeset and Hillerborg [6]. (b) Samani and Attard [7]. (c) This study.

deviation of the NRMSE, respectively. It is noteworthy that the comparisons of test results with the predictions of Markeset and Hillerborg [6] were conducted only in the descending branch because Markeset and Hillerborg's model [6] provides the equations only for the descending branch behavior.

Markeset and Hillerborg [6] idealized the CDZ model considering fracture energy and proposed the descending branch behavior in the stress-strain relationship. In the CDZ model, the total strain is a combination of the strain (ε) in the region where the undamaged zone elastically unloads after the peak stress, the strain (ε_d) in the region propagated by the longitudinal microsplitting cracks, and the strain (ω/h) by the diagonal tensile band crack. In the model, ε_d is based on the assumption that inelastic deformation in the damaged zone determines the descending branch behavior. To consider inelasticity in the descending branch, ε_d introduces $((f'_c - f_c)/f'_c)^{0.8}$ as that expressed in equation (8); nevertheless, the descending branch is predicted as a virtually linear curve (Figure 10(a)). However, the shapes of the descending branch measured in the existing test results are primarily curved rather than linear. Hence, the accuracy of Markeset and Hillerborg's model [6] according to the concrete type fluctuates with large deviations. The values of γ_m obtained by Markeset and Hillerborg's model [6] are 0.39 for LWC, 0.29 for NWC, and 0.29 for HWC. In particular,

Table 3: Comparisons of normalized root-mean-square error.

Concrete type	Aspect ratio	Statistical value	Researcher		
			Markeset and Hillerborg [6]	Samani and Attard [7]	This study
LWC	1	γ_m	0.50	0.45	0.21
		γ_s	0.35	0.11	0.10
	2	γ_m	0.28	0.38	0.27
		γ_s	0.24	0.17	0.24
	Subtotal	γ_m	0.39	0.41	0.24
		γ_s	0.13	0.29	0.16
NWC	0.5~1.0	γ_m	0.32	0.24	0.13
		γ_s	0.12	0.07	0.02
	2~3.5	γ_m	0.29	0.22	0.17
		γ_s	0.16	0.16	0.11
	4.0~8.0	γ_m	0.24	0.34	0.39
		γ_s	0.03	0.03	0.05
	Subtotal	γ_m	0.29	0.23	0.19
		γ_s	0.14	0.14	0.12
HWC	2.0	γ_m	0.29	0.73	0.10
		γ_s	0.14	0.09	0.01
Total		γ_m	0.32	0.34	0.19
		γ_s	0.19	0.21	0.13

Markeset and Hillerborg's model [6] underestimates the compressive stress of HWC. This is because this model does not consider the decreasing effect of the slope for HWC in the descending branch because the factor of k to determine ε_d according to concrete type is 3 and 1, only for NWC and LWC, respectively, without considering HWC.

Samani and Attard [7] applied the size effect to the equations for the descending branch proposed by Attard and Setunge's model [11]. As summarized in Table 2, the descending branch behavior proposed by Samani and Attard [7] is also based on the CDZ model and its strain equation is similar to that of Markeset and Hillerborg' s model [6]. In addition, Markeset and Hillerborg's model [6] for ε_d composed of functions of k, γ, and G_F is used without modification. The descending branch behavior in Samani and Attard's model [7], however, is different from that in Markeset and Hillerborg [6], indicating that it is predicted as a curve with an inflection point. As shown in Figure 10(b), the ascending branch behavior composed of functions f'_c and ρ_c in Samani and Attard's model [7] is identical to that in Attard and Setunge's model [11]. In the descending branch behavior of Samani and Attard's model [7], the increasing effect of the decreasing slope is explained well with the increase in h/d_{eq}, as shown in Figure 10(b). However, Samani and Attard's model [7] underestimates the compressive stress for HWC. This is because, in this model, the factor k related with the material property does not consider the decreasing effect of the descending slope for HWC. This implies that the factor k in Samani and Attard's model [7] requires calibration using additional test results. In addition, because Samani and Attard's model [7] does not consider the size effect on the peak stress, it overestimates the compressive strength of concrete for LWC. The overestimation increased with the increase in d_{eq}. The values of γ_m obtained by Samani and Attard's model [7] are 0.41 for LWC, 0.23 for NWC, and 0.73 for HWC.

The proposed model in this study shows better agreement with test results, irrespective of d_{eq}, h/d_{eq}, concrete type, and f'_c. The values of γ_m and γ_s are 0.24 and 0.16 for LWC, 0.19 and 0.12 for NWC, and 0.10 and 0.01 for HWC, respectively. The results are lower than those of the models of Markeset and Hillerborg [6] and Samani and Attard [7]. The proposed values of γ_m and γ_s are 0.19 and 0.13, respectively, which are the lowest among other models. Based on the CDZ model, a rational stress-strain model for unconfined concrete considering the size effect is proposed, using the key parameter β_1 formulated by functions of f'_{SE}, d_{eq}, h/d_{eq}, and ρ_c. Note that most tests to investigate the stress-strain curves of concrete in compression were conducted using standard cylindrical specimens of 100×200 mm or 150×300 mm. Moreover, very few specimens with the equivalent diameter exceeding 200 mm are available in the literatures because of the capacity limitation of the testing machine. Thus, the proposed models need to be further examined in LWC and HWC specimens with a larger size.

5. Conclusions

From the proposed stress-strain relationship model for various unconfined concrete types considering the size effect based on the CDZ model, the following conclusions were derived:

(1) Although the concrete commonly has microcracks, the elastic modulus of concrete typically defined as $0.4f'_c$ where bond cracks occurred in was not affected by the size effect, whereas the strain at the peak stress was affected by the size effect because of propagation of cracks.

(2) $\varepsilon_{SE0.5} - (\varepsilon_{SE} - f'_{SE}/E_c)$ that closely related to the slopes of descending branches in stress-strain relationship decreased averagely by 25% and 43%,

respectively, when equivalent diameter and aspect ratio increased by 3 times. The corresponding values for lightweight concrete (LWC) were lower than those for normal weight concrete (NWC) and heavyweight concrete (HWC).

(3) The key parameter β_1 determining the slope of the ascending and descending branches could be proposed as an exponential function of $(f'_{SE}/10)(2300/\rho_c)^{1.5}$ and $(f'_{SE}/10)^{0.65}(d_{eq}/150)^{0.2}\ (h/d_{eq})^{0.4}(2300/\rho_c)^{1.2}$, respectively.

(4) The proposed model of the stress-strain relationship for unconfined concrete showed good agreements with the test results, irrespective of equivalent diameter and aspect ratio of specimen, concrete density, and compressive strength.

Notations

d_{eq}: Equivalent diameter
d_a: Maximum size of aggregate
h: Height of specimen
h/d_{eq}: Aspect ratio of specimen
h_0: Reference height of specimen
h_d: Damage zone height of specimen
E_0: Secant modulus at the peak stress
E_c: Elastic modulus of concrete
E_t: Strain-softening modulus
f_c: Stress at stress-strain curve
f'_c: Compressive strength of concrete measured in the standard specimen
f_{ic}: Inflection stress in descending branch
f'_{SE}: Compressive strength concrete considering the size effect
G_F: Fracture energy
k: Factor relating to material property
k_1: Conversion coefficient
n: Number of microcracks in the band
W^{in}: Amount of energy released in the unloading zones
X_1, X_2, X_3, and X_4: Experimental constants
α_1, α_2: Modification functions to account for the volume of the crack band zone
β_1: Key parameter that determines the slope of ascending and descending branches
γ: Factor relating to height of specimen
γ_m: Mean of normalized root-mean-square error
γ_s: Standard deviation of normalized root-mean-square error
ε: Strain induced from elastically unloading in the undamaged zone
$\varepsilon_{0.5}$: Strain at $0.5f'_c$ after the peak stress
ε_0: Stain at the peak stress
ε_c: A strain at stress-strain curve
ε_d: Strain in the damaged zone relating to longitudinal microsplitting cracking
ε_h: Total strain occurred in compression damage zone (CDZ)
ε_{ic}: Strain at inflection stress in descending branch
ε_{SE}: Strain at the peak stress considering the size effect
$\varepsilon_{SE0.5}$: Strain at $0.5f'_{SE}$ after the peak stress
μ_1: Factor relating to type of coarse aggregate
ρ_c: Concrete density
χ: Coefficient to account for the relation of E_0 and E_c
ω: Localized deformation
ω/h: Strain of diagonal tensile shear band.

Data Availability

The data records used to support the findings of this study are included within the article.

Conflicts of Interest

The authors declare that there are no conflicts of interest regarding the publication of this paper.

Acknowledgments

This research was supported by the research grant from Kyonggi University through the Korea Agency for Infrastructure Technology Advancement funded by the Ministry of Land, Infrastructure and Transport of the Korean Government (Project no. 19TBIP-C126470-03).

References

[1] K. H. Yang, J. H. Mun, M. S. Cho, and T. H.-K. Kang, "Stress-strain model for various unconfined concretes in compression," *ACI Structural Journal*, vol. 111, no. 4, pp. 819–826, 2014.

[2] T. H. Almusallam and S. H. Alsayed, "Stress-strain relationship of normal, high-strength and lightweight concrete," *Magazine of Concrete Research*, vol. 47, no. 170, pp. 39–44, 1995.

[3] B.-I. Bae, H.-K. Choi, B.-S. Lee, and C.-H. Bang, "Compressive behavior and mechanical characteristics and their application to stress-strain relationship of steel fiber-reinforced reactive powder concrete," *Advances in Materials Science and Engineering*, vol. 2016, Article ID 6465218, 11 pages, 2016.

[4] D. C. Jansen and S. P. Shah, "Effect of length on compressive strain softening of concrete," *Journal of Engineering Mechanics*, vol. 123, no. 1, pp. 25–35, 1997.

[5] J.-I. Sim, K.-H. Yang, H.-Y. Kim, and B.-J. Choi, "Size and shape effects on compressive strength of lightweight concrete," *Construction and Building Materials*, vol. 38, pp. 854–864, 2013.

[6] G. Markeset and A. Hillerborg, "Softening of concrete in compression—localization and size effects," *Cement and Concrete Research*, vol. 25, no. 4, pp. 702–708, 1995.

[7] A. K. Samani and M. M. Attard, "A stress–strain model for uniaxial and confined concrete under compression," *Engineering Structures*, vol. 41, pp. 335–349, 2012.

[8] Z. P. Bažant and J. Planas, *Fracture and Size Effect in Concrete and Other Quasibrittle Materials*, CRC Press, New York, NY, USA, 1998.

[9] Z. P. Bažant, "Size effect in blunt fracture: concrete, rock, metal," *Journal of Engineering Mechanics*, vol. 110, no. 4, pp. 518–535, 1984.

[10] J.-K. Kim and S. H. Eo, "Size effect in concrete specimens with dissimilar initial cracks," *Magazine of Concrete Research*, vol. 42, no. 153, pp. 233–238, 1990.

[11] M. Attard and S. Setunge, "Stress-strain relationship of confined and unconfined concrete," *ACI Materials Journal*, vol. 93, no. 5, pp. 432–442, 1996.

[12] R. Vonk, *Softening of Concrete Loaded in Compression*, Ph.D. thesis, Eindhoven University of Technology, Eindhoven, Netherlands, 1992.

[13] K. H. Lee, K. H. Yang, J. H. Mun, and S. J. Kwon, "Mechanical properties of concrete made from different expanded lightweight aggregates," *ACI Materials Journal*, 2018, In press.

[14] J.-S. Mun, J.-H. Mun, K.-H. Yang, and H. Lee, "Effect of substituting normal-weight coarse aggregate on the workability and mechanical properties of heavyweight magnetite concrete," *Journal of the Korea Concrete Institute*, vol. 25, no. 4, pp. 439–446, 2013, in Korean.

[15] G. Muciaccia, G. Rosati, and G. Di Luzio, "Compressive failure and size effect in plain concrete cylindrical specimens," *Construction and Building Materials*, vol. 137, pp. 185–194, 2017.

[16] A. Neville, *Properties of Concrete*, Pearson Education Limited, Harlow, UK, 5th edition, 2011.

[17] M. A. Taylor and B. B. Broms, "Shear bond strength between coarse aggregate and cement paste or mortar," *ACI Proceedings*, vol. 61, no. 8, pp. 939–958, 1964.

[18] T. Noguchi, F. Tomosawa, K. M. Nemati, B. M. Chiaia, and A. P. Fantilli, "A practical equation for elastic modulus of concrete," *ACI Structural Journal*, vol. 106, no. 5, pp. 690–696, 2009.

[19] P. T. Wang, S. P. Shah, and A. E. Naaman, "Stress-strain curves of normal and lightweight concrete in compression," *ACI Journal Proceedings*, vol. 75, no. 11, pp. 603–611, 1978.

[20] K. H. Yang and J. I. Sim, "Modeling of the mechanical properties of structural lightweight concrete based on size effects," Technical Report, Department of Plant•Architectural Engineering, Kyonggi University, Suwon, Republic of Korea, 2011, in Korean.

[21] H. C. Mertol, S. J. Kim, A. Mirmiran, S. Rizkalla, and P. Zia "Behavior and design of HSC members subjected to axial-compression and flexure," in *Proceedings of the 7th International Symposium on Utilization of High-Strength/High–Performance Concrete (SP-228)*, H. G. Russell, Ed., pp. 395–420, American Concrete Institute, Washington, DC, USA, 2005.

[22] M. H. Zhang and O. E. Gjørv, "Mechanical properties of high strength lightweight concrete," *ACI Materials Journal*, vol. 88, no. 3, pp. 240–247, 1991.

[23] K. H. Yang, J. S. Mun, and H. Lee, "Workability and mechanical properties of heavyweight magnetite concrete," *ACI Materials Journal*, vol. 111, no. 3, pp. 273–282, 2014.

[24] T. H. Wee, M. S. Chin, and M. A. Mansur, "Stress-strain relationship of high-strength concrete in compression," *Journal of Materials in Civil Engineering*, vol. 8, no. 2, pp. 70–76, 1996.

[25] A. H. Nilson, "High–strength concrete: an overview of Cornell research," in *Proceedings of Symposium on Utilization of High–Strength Concrete*, pp. 27–37, Stavanger, Norway, June 1987.

[26] S.-T. Yi, J.-K. Kim, and T.-K. Oh, "Effect of strength and age on the stress-strain curves of concrete specimens," *Cement and Concrete Research*, vol. 33, no. 8, pp. 1235–1244, 2003.

[27] T. C. Liu, *Stress–Strain Response and Fracture of Concrete in Biaxial Compression*, Cornell University, Ithaca, NY, USA, 1971.

[28] A. Tomaszewicz, "Betongens arbeidsdiagram," SINTEF Report No. STF 65A84065, SINTEF, Trondheim, Norway, 1984.

[29] J. H. Mun, J. S. Mun, and K. H. Yang, "Stress–strain relationship of heavyweight concrete using magnetite aggregate," *Journal of Architectural Institute of Korea*, vol. 29, no. 8, pp. 85–92, 2013, in Korean.

[30] Comité Euro-International du Beton (CEB-FIP), *Structural Concrete: Textbook on Behaviour, Design and Performance*, International Federation for Structural Concrete (fib), Lausanne, Switzerland, 1999.